Chapter 7

Summary, outlook and conclusions

7.1 First-generation experiments

7.1.1 Virtual bremsstrahlung

The well-known coupling of the photon with the nucleon together with the fact that photons (or any electromagnetic (e.m.) probe) interact only relatively weakly with nucleons, make bremsstrahlung production an ideal tool to study details of the nucleon-nucleon interaction. In this thesis dilepton production (e^+e^-) in proton-proton scattering, $pp \rightarrow ppe^+e^-$, and proton-deuteron capture, $p+d \rightarrow {}^3\mathrm{He}+e^+ +e^-$, has been discussed. According to quantum electrodynamics (QED), the dileptons in these reactions can be described by the emission of a massive virtual photon. Consequently, these processes add new information to what can already be obtained by studying real-photon production. First of all, a virtual photon can be longitudinally polarized, and therefore adds an additional degree of freedom to those of a real photon, which is limited to transverse polarizations. Secondly, the coupling of the virtual photon to the dileptons makes it experimentally possible to decompose the nucleonic current into different components (response functions) which are related to the emission of virtual photons with different polarization states. The transverse components can also be obtained with reactions involving real photons by measuring their polarizations. However, at photon energies discussed in this thesis (50-130 MeV), this has not been experimentally achieved so far.

7.1.2 Experiment

The difficulty in experimentally observing the bremsstrahlung reaction is related to its small cross section. The cross section of the elastic pp reaction is in the order of 10 mb, whereas the cross section for real-photon production in proton-proton scattering is only $\approx 1\ \mu b$. Due to the additional e.m. coupling of the photon to a lepton pair, the cross section for virtual bremsstrahlung is even a factor $\alpha \approx 1/137$ smaller than the already small cross section for real-photon production. Experimentally, it is therefore required to have high luminosities and a detector system with a large acceptance and efficiency. The detector should be able to handle the high counting rates resulting from the elastic channel and should provide means to suppress the background to a negligible level.

In this thesis we have outlined an experimental procedure in which it is clearly demonstrated that it is possible to study experimentally with a reasonable amount of statistics and nearly

background-free the virtual-bremsstrahlung reactions, $pp \to ppe^+e^-$ and $pd \to {}^3\mathrm{He}\,e^+e^-$. The experimental setup consists of a hadron detector, SALAD, and the photon/lepton spectrometer, TAPS, which are operated in a coincidence mode. With this setup the positions and energies of all final-state particles are determined with sufficient resolution and with a large coverage of the total solid angle. A high luminosity was obtained by using a liquid hydrogen/deuterium target in combination with a 190 MeV proton beam with an average intensity of 6 nA.

7.1.3 Analysis

In the off-line analysis it is shown that $pp \to ppe^+e^-$ and $pd \to {}^3\mathrm{He}\,e^+e^-$ events can be obtained with negligible "background". For the $pp \to ppe^+e^-$ event selection, we have selected those events for which at least two proton tracks were identified by the SALAD detector (2 multi-wire proportional chamber hits plus a corresponding scintillator response) in coincidence with at least two charged e.m. showers in TAPS, corresponding to electrons or positrons. The selection of the $pd \to {}^3\mathrm{He}\,e^+e^-$ events was performed similarly, except that for this channel at least one wire-chamber track, corresponding to the ^{3}He, was required. In the p+p and p+d experiments we measured more observables than needed to define the momenta and energies of all outgoing particles of the $pp \to ppe^+e^-$ and $pd \to {}^3\mathrm{He}\,e^+e^-$ processes, respectively. Together with the excellent time resolution of the BaF_2 crystals and the use of charged-particle counters to discriminate between real and virtual photons, these extra observables have been exploited such as to reduce the background to a negligible level without a significant loss of good $pp \to ppe^+e^-$ and $pd \to {}^3\mathrm{He}\,e^+e^-$ events. For the $pp \to ppe^+e^-$ reaction we have obtained a total of 600 events and for the $pd \to {}^3\mathrm{He}\,e^+e^-$ reaction a total of 320 events.

7.1.4 Differential cross sections

Normalization

Differential cross sections were experimentally obtained for both reactions. For this we have corrected the selected $pp \to ppe^+e^-$ and $pd \to {}^3\mathrm{He}\,e^+e^-$ events for the individual detector efficiencies (including wire-chamber, trigger, and CPC efficiencies) and the luminosity. For the $pp \to ppe^+e^-$ experiment, the luminosity was obtained by measuring concurrently throughout the complete experiment the elastic pp yield, which is then normalized to the well-known elastic cross section. The luminosity thus obtained has been compared with the nominal luminosity calculated from the nominal target thickness and the total collected charge in a Faraday cup, and is found to differ by 25%. The latter is explained by the bulging of the LH_2 target and uncertainties in the calibration of the Faraday cup. The luminosity in the p+d experiment is obtained by using the information of the Faraday cup and the nominal target thickness, plus the additional correction of 30±5% which is estimated by averaging the correction found in the p+p experiment in the "supercluster" and in the "block" geometry. For the $pp \to ppe^+e^-$ and the $pd \to {}^3\mathrm{He}\,e^+e^-$ reaction a systematical uncertainty of ±15% and ±20%, respectively, is obtained.

Results for the $pp \to ppe^+e^-$ reaction

For the first time differential cross sections as a function of the invariant mass, M_γ, and the polar angle of the virtual photon, θ_γ, have been obtained for the $pp \to ppe^+e^-$ reaction below

the pion-production threshold. The data are compared with two types of models: low-energy calculations (LETs) and a microscopic model.

The low-energy calculations are derived by Korchin et al. [Kor95, Kor96]. These approximations express the virtual-bremsstrahlung amplitude in terms of the elastic pp process and the static properties (mass, charge and magnetic moment) of the proton. In practice this is achieved by first calculating the external diagrams (the virtual photon coupling to the external legs of the protons) within an expansion around the on-shell kinematics. Re-scattering and meson-exchange currents are partially taken into account by adding to the external amplitude a so-called internal amplitude, which is obtained by imposing gauge invariance. The internal amplitude, however, is not uniquely defined, which therefore leads to different low-energy calculations. In this thesis two such calculations are presented. For the kinematics involved in our experiment (photon energies between 50-80 MeV), the predicted cross sections of the two approximations differ by 30%, indicating that in our case the validity of the low-energy approximations is rather doubtful.

The second type of model presented in this thesis is a fully-relativistic microscopic calculation developed by Martinus et al. [Mar97a, Mar98]. This model applies a scattering T-matrix to the virtual-bremsstrahlung process, including relativistic and off-shell effects of the nucleon-nucleon interaction. This scattering matrix is obtained by solving the Lippmann-Schwinger equation with as input a one-boson exchange potential developed by Fleischer and Tjon [Fle74, Fle77, Fle80]. Furthermore, meson-exchange and Δ contributions are added perturbatively to the amplitude.

All models have been implemented in a Monte-Carlo event generator. Together with the use of the detector-simulation package GEANT3 [Bru86], simulated data were generated and analyzed identically to the experimental data. In this way, the measured cross sections are directly compared with the predictions of the models without unfolding the experimental data by the detector acceptances.

The shape of the $pp \rightarrow ppe^+e^-$ cross section as function of M_γ and θ_γ is reasonably well described by all models (see figs 5.16,5.17). It has to be remarked that the shape of the invariant-mass distribution is primarily dominated by a $1/M_\gamma$ dependence resulting from a phase-space term in combination with a propagation term of the virtual photon. The shape of the measured polar-angle distribution of the virtual photon is primarily dominated by the detector acceptance. Surprisingly, the microscopic model overestimates the experimental data by a factor of two. To a lesser extent a similar effect has also been observed for real bremsstrahlung yields [Hui99]. It is clear that the microscopic model needs improvement. Part of the discrepancy with the microscopic model resides in the fact that the NN potential of references [Fle74, Fle77, Fle80] does not provide a good fit to the present-day NN database. However, the discrepancy between data and calculation is too large to be explained completely by this problem. Remaining problems in the model could be either the missing of higher-order effects not taken explicitly into account or the approximations made in modeling the off-shell NN interaction. Also remarkable is the good description of the data by one of the low-energy models (VL): for the large photon energies (50-80 MeV) involved in our experiment, the validity of these types of calculations is doubtful.

Results for the $pd \to {}^3\mathrm{He}\, e^+e^-$ reaction

Also for the $pd \to {}^3\mathrm{He}\, e^+e^-$ experiment, differential cross sections as function of the invariant mass and the polar angle of the virtual photon have been obtained. Different from the $pp \to ppe^+e^-$ reaction, the acceptance of the detector has been unfolded from the $pd \to {}^3\mathrm{He}\, e^+e^-$ data. These results extend the measurements performed at Uppsala with the dilepton spectrometer PACMAN [Joh98]. In that experiment cross sections for virtual-photon masses smaller than 8 MeV and at two polar angles of the virtual photon, namely $\theta_\gamma^{\mathrm{cm}}$=48° and $\theta_\gamma^{\mathrm{cm}}$=92°, were measured at an incoming proton energy of 178 MeV. The experiment discussed in this thesis has determined the differential cross section of the $pd \to {}^3\mathrm{He}\, e^+e^-$ reaction for virtual-photon masses M_γ>15 MeV and at polar angles of the virtual photon between 80°<$\theta_\gamma^{\mathrm{cm}}$<140° and a proton energy of 190 MeV.

This thesis also discusses the analysis of real-photon production in proton-deuteron capture, p+d→^{3}He+γ, which has been measured concurrently with the $pd \to {}^3\mathrm{He}\, e^+e^-$ reaction during the same experiment. For the $pd \to {}^3\mathrm{He}\,\gamma$ reaction, the differential cross section as function of $\theta_\gamma^{\mathrm{cm}}$ has been obtained for polar angles in the center-of-mass frame, $\theta_\gamma^{\mathrm{cm}}$, between 80°-140° and for a proton beam energy of 190 MeV. Our data is in good agreement with previously published data [Pic87, Joh98, Sch97a].

The differential cross sections of the $pd \to {}^3\mathrm{He}\,\gamma$ and $pd \to {}^3\mathrm{He}\, e^+e^-$ data, have been compared with a gauge-invariant impulse approximation developed by Korchin et al. [Kor98, Kor99]. Similar to the LET models used to predict the $pp \to ppe^+e^-$ reaction, this calculation exploits also current conservation to obtain an internal amplitude. The latter is supposed to take partially into account re-scattering diagrams and meson-exchange contributions. In contrast to the LET calculations, in this model the external contributions are calculated explicitly, i.e. without an expansion towards small photon energies[1]. The ^{3}He wave function is obtained by applying the recent Argonne V18 nucleon-nucleon potential together with the Urbana IX three-nucleon interaction [For96]. The gauge-invariant model has been compared with the existing world data set for real-photon production in proton-deuteron capture for incoming proton energies varying between 100 and 500 MeV [Kor98]. It was noted that in general at backward photon angles the calculation underestimates the world data set. To account for this discrepancy, an energy-dependent correction factor for the self-energy of the ^{3}He was introduced. As was shown in section 3.3.2, this correction is equivalent to an off-shell modification of the anomalous magnetic moment of the ^{3}He, κ, by $\kappa_{\mathrm{eff}}=\kappa(1+\xi(E))$, where ξ is the modification factor and its value is obtained by fitting the calculation to the experimental data. At 200 MeV the fit to the world database was improved significantly by taking ξ=1.3, corresponding to a modification of the anomalous magnetic moment of the ^{3}He by a factor of 2.3. A similar discrepancy between data and the calculation has been observed in the $pd \to {}^3\mathrm{He}\,\gamma$ experiment discussed in this thesis. We note that in our analyses the fitted value for ξ is: 1.20±0.15(stat.)±0.30(sys.). Also for the $pd \to {}^3\mathrm{He}\, e^+e^-$ data, we found that a similar modification of ξ=1.2 was necessary to minimize the discrepancy between calculation and data. Theoretically, it would be interesting to confirm whether a microscopic approach can explain this effect.

Furthermore, we have studied the ratio, R, between the virtual- and real-photon yields. Experimentally, the advantage of this new observable, R, is that common systematical uncertainties cancel. Theoret
aspects in the reaction me
virtual-photon production.
enhancement of 35% in the
is found at θ_γ=48° for virtua
at somewhat different kinen
predictions of the gauge-inva

7.1.5 Response functi

With the TAPS detector th
sured. Therefore, the depend
and azimuthal angles, θ_ℓ an
This allows an experimental
(response functions) W_T, W
corresponding polarization o
transverse (TT,TT') and lon
we have presented the first d
production in proton-proton
measurements are mainly a f

The first problem we en
$^3\mathrm{He}\, e^+e^-$ events collected. T
specific kinematics. Instead w
tal coverage. Consequently,
$\overline{W}_{LT}$, $\overline{W'}_{TT}$ and $\overline{W'}_{LT}$ as de
over a large part of the phase
which show up at specific kin

The second problem is th
our experiment. This influen
functions (W_{TT},W_{LT},W'_{TT} an
shown that the averaged interf
upon the response function W_i
covered experimentally, the res
functions. In order to subtract
needs to introduce a model, a

For the $pp \to ppe^+e^-$ reac
them with the predictions of
model. The response functions
to account for the discrepancy f
the microscopic model gives a r
response functions. Only at la
can be observed for $\overline{W}_{TT}$ and

Also for the $pd \to {}^3\mathrm{He}\, e^+e$
response functions $\overline{W}_T$, $\overline{W}_L$,
gauge-invariant impulse approx

[1] Note that the energy of the photon in the pd-capture process in the center-of-mass frame is equal to 130 MeV, which is larger than in pp scattering

[2] For the $pd \to {}^3\mathrm{He}\, e^+e^-$ process W

certainties cancel. Theoretically this observable is of interest because it points directly to aspects in the reaction mechanism of the $pd \rightarrow {}^3\mathrm{He}\, e^+e^-$ process which are not present in virtual-photon production. In the experiment with the dilepton spectrometer PACMAN an enhancement of 35% in the ratio between the virtual-photon yield and the real-photon process is found at θ_γ=48° for virtual-photon masses M_γ<8 MeV [Joh98]. However, in our experiment at somewhat different kinematics, this ratio R does not show any significant deviations from predictions of the gauge-invariant impulse approximation.

7.1.5 Response functions

With the TAPS detector the momenta of the outgoing leptons ($\mathbf{k}_+$ and $\mathbf{k}_-$) have been measured. Therefore, the dependence of the cross section on the invariant mass, M_γ, and the polar and azimuthal angles, θ_ℓ and ϕ_ℓ, of the momentum vector $\ell=\frac{1}{2}(k_+ - k_-)$ could be studied. This allows an experimental decomposition of the reaction amplitude into a set of observables (response functions) W_T, W_L, W_{TT}, W_{LT}, W'_{TT} and W'_{LT}, where the labeling indicates the corresponding polarization of the virtual photon: transverse (T), longitudinal (L), transverse-transverse (TT,TT') and longitudinal-transverse (LT,LT') interference terms. In this thesis we have presented the first determination of the response functions for virtual-bremsstrahlung production in proton-proton scattering and proton-deuteron capture. These first-generation measurements are mainly a feasibility study for experimentally extracting response functions.

The first problem we encountered is the small number of $pp \rightarrow ppe^+e^-$ and $pd \rightarrow {}^3\mathrm{He}\, e^+e^-$ events collected. Therefore, we were not able to study the response function for specific kinematics. Instead we were forced to integrate the data over the accepted experimental coverage. Consequently, we introduced the averaged response functions $\overline{W}_T$, $\overline{W}_L$, $\overline{W}_{TT}$, $\overline{W}_{LT}$, $\overline{W'}_{TT}$ and $\overline{W'}_{LT}$ as defined in eqs (5.13),(5.15), (5.16). Unfortunately, by integrating over a large part of the phase space, one loses specific sensitivity to details of the interaction which show up at specific kinematics.

The second problem is the incomplete experimental coverage of the dihedral angle ϕ_ℓ in our experiment. This influences in particular the determination of the interference response functions (W_{TT},W_{LT},W'_{TT} and W'_{LT}). In case of a complete coverage of ϕ_ℓ, it can easily be shown that the averaged interference response functions, $\overline{W}_i$ (i=TT,LT,TT',LT'), only depend upon the response function W_i itself. However, in case the dihedral angle, ϕ_ℓ, is not completely covered experimentally, the response functions $\overline{W}_i$ are in general a mixture of all other response functions. In order to subtract the contributions of the non-vanishing response functions, one needs to introduce a model, and therefore the results are model dependent.

For the $pp \rightarrow ppe^+e^-$ reaction we have studied all six response functions, and compared them with the predictions of one of the low-energy calculations (VL) and of the microscopic model. The response functions of the microscopic model have been normalized by a factor 0.55 to account for the discrepancy found in the differential cross section. Within this normalization, the microscopic model gives a reasonable description of all experimentally-determined averaged response functions. Only at large virtual-photon masses deviations (one standard deviation) can be observed for $\overline{W}_{TT}$ and $\overline{W}_{LT}$. The same holds for the low-energy calculation.

Also for the $pd \rightarrow {}^3\mathrm{He}\, e^+e^-$ reaction, we have experimentally determined four averaged response functions $\overline{W}_T$, $\overline{W}_L$, $\overline{W}_{TT}$ and $\overline{W}_{LT}$.[2] These results have been compared to the gauge-invariant impulse approximation with the modification of the magnetic moment of the

[2] For the $pd \rightarrow {}^3\mathrm{He}\, e^+e^-$ process W'_{TT}=W'_{LT}=0 (see section 2.2.3).

^{3}He. In general, the model gives a reasonable description of the data. There are two exceptions. A sign change of the response function, $\overline{W}_{TT}$, at low invariant masses by going from small virtual-photon polar angles ($70°<\theta_\gamma^{cm}<105°$) towards larger virtual-photon angles ($120°<\theta_\gamma^{cm}<145°$) has been measured, which, curiously enough, is predicted by the model with the wrong sign. Furthermore, for the same virtual-photon masses at $70°<\theta_\gamma^{cm}<105°$, $\overline{W}_{LT}$ seems to be overestimated by the model predictions.

7.2 Second-generation experiments

7.2.1 Introduction

The work presented in this thesis has clearly demonstrated that measuring the virtual-bremsstrahlung yields in few-body systems, like proton-proton scattering or proton-deuteron capture, is possible. Furthermore, it has been shown that the determination of the response functions becomes feasible. In chapter 3 the advantage of studying the individual response functions was discussed. In particular it was shown that higher-order contributions, i.e. negative-energy states and two-body currents, can be experimentally studied by measuring different response functions (see fig. 3.11). It is however necessary to have a good statistical accuracy in order to observe these higher-order contributions. The experiment discussed in this thesis has not provided enough events to be sensitive to these contributions. For a successful determination of the interference response functions, a complete coverage of the dihedral angle ϕ_ℓ is necessary.

At KVI, second-generation experiments are planned to study the virtual-bremsstrahlung production in proton-proton scattering and proton-deuteron capture. These measurements should meet the above mentioned requirements for as complete as possible coverage of the solid angle and especially of the dihedral angle ϕ_ℓ. For this, a spherical detector covering 80% of the 4π solid angle, the Plastic Ball [Bad82], will be used for the detection of the e^+e^- pair. The detector consists of more than 600 phoswich elements. Each element is a plastic scintillator optically coupled to a thin slice of CaF_2 crystal. Monte-Carlo simulations [Sch99b] predict this instrument to be $\approx$30% efficient for detecting both leptons emitted from the inelastic pp process.

7.2.2 $pp \rightarrow ppe^+e^-$

For the $pp \rightarrow ppe^+e^-$ experiment, the Plastic Ball will be used in coincidence with the SALAD detector. With this setup, it is predicted that more than 200.000 $pp \rightarrow ppe^+e^-$ events will be obtained within a measuring period of 500 hours. To illustrate the accuracy one obtains with this experiment, we have plotted in figs. 7.1 and 7.2, the averaged response functions $\overline{W}_T$, $\overline{W}_L$, $\overline{W}_{TT}$ and $\overline{W}_{LT}$. These results are obtained by a Monte-Carlo simulation using the VL low-energy model. In this simulation a total of 100.000 $pp \rightarrow ppe^+e^-$ events have been used. The error bars in the figures represent the statistical accuracy. In the top panel of fig. 7.1 events are selected for which $\theta_\ell<10°$. The cut on the energy-sharing angle, θ_ℓ, is applied in order to minimize the contribution from W_L (dashed line). Note that due to the complete coverage of ϕ_ℓ the contribution from the interference response functions become zero. In the bottom panel of fig. 7.1, the predictions for $\theta_\ell>80°$ are plotted. With this constraint the longitudinal response can be observed over the whole virtual-photon mass range. Note that the statistical uncertainty of the simulated data is sufficiently small to observe the effect of the longitudinal

response.

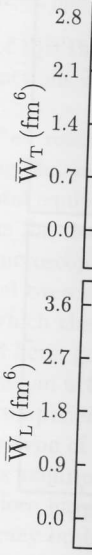

Figure 7.1: *Shown is the acc*
$\overline{W}_L$. *These predictions are ob*
are selected for which the en
the contribution from W_T *and*
(dotted line) which is obtained

In fig. 7.2 the predicted re
$\overline{W}_{LT}$, which are obtained by
respectively. Due to a complet
Note the remarkable high-pre
subtraction procedure.

For the simulated data sho
space for proton angles $6°<\theta_p$
the good accuracy one achiev
functions at several kinematics

A polarized-proton beam i
ton polarization is determined,
coefficients. To do so requires
for superior statistics. The dat
presented in this thesis are not
of accuracy. It is expected th
virtual-photon yields with the s

response.

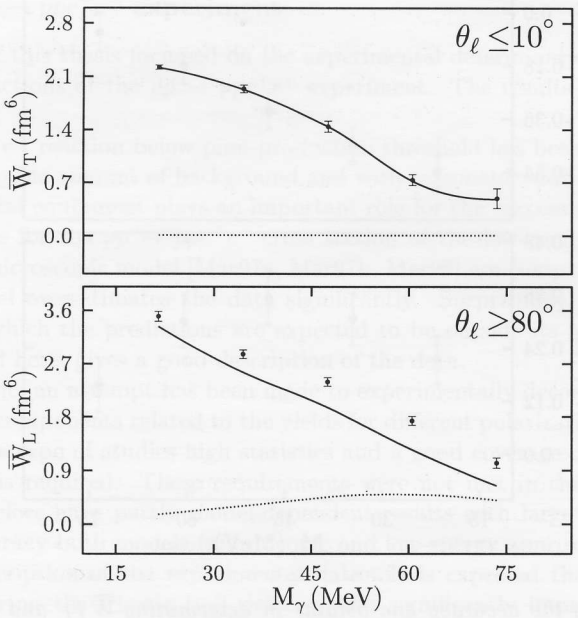

Figure 7.1: *Shown is the accuracy one obtains with 100.000 pp $\rightarrow$ ppe^+e^- events for $\overline{W}_T$ and $\overline{W}_L$. These predictions are obtained with the Virtual-photon Low model. In the top panel events are selected for which the energy-sharing angle θ_ℓ<10°. The solid and dotted lines represent the contribution from W_T and W_L, respectively. The bottom panel shows the sensitivity to W_L (dotted line) which is obtained by selecting events with θ_ℓ>80°.*

In fig. 7.2 the predicted results are shown for the interference response functions $\overline{W}_{TT}$ and $\overline{W}_{LT}$, which are obtained by measuring the $\cos 2\phi_\ell$ and $\cos \phi_\ell$ amplitudes of the cross section, respectively. Due to a complete coverage of ϕ_ℓ all remaining contributions are reduced to zero. Note the remarkable high-precision one can obtain without the need for a model-dependent subtraction procedure.

For the simulated data shown here, we have explicitly integrated over the complete phase space for proton angles $6^\circ < \theta_p < 26^\circ$ to compare with the data discussed in this thesis. Within the good accuracy one achieves with 100.000 events, the possibility to study the response functions at several kinematics becomes therefore possible.

A polarized-proton beam in combination with virtual bremsstrahlung, whereby the photon polarization is determined, allows the experimental measurement of polarization-transfer coefficients. To do so requires very accurate data to be obtained from experiments aiming for superior statistics. The data from the first generation virtual-bremsstrahlung experiments presented in this thesis are not suitable for extracting these observables with a sufficient degree of accuracy. It is expected that due to the good accuracy one achieves in determining the virtual-photon yields with the second-generation experiments, the measurement of this type of

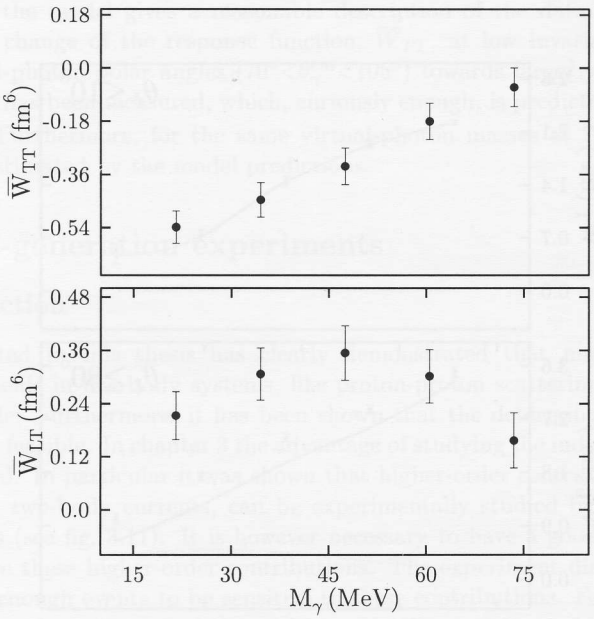

Figure 7.2: *Shown is the accuracy one obtains in determining $\overline{W}_{TT}$ and $\overline{W}_{LT}$ with 100.000 $pp \to ppe^+e^-$ events. The error bars on the data points (filled dots) are the statistical uncertainties.*

polarization observables becomes feasible.

7.2.3 $pd \to {}^3\mathrm{He}\, e^+e^-$

To study the response functions and cross sections of the $pd \to {}^3\mathrm{He}\, e^+e^-$ reaction with much better accuracies than the experiment presented in this thesis, it is planned to place the Plastic Ball in coincidence with the Big-Bite Spectrometer (BBS) [Ber95]. The latter instrument measures the ^{3}He at small forward angles down to $\theta_{^3\mathrm{He}}$=0°, whereas the SALAD detector is limited to $\theta_{^3\mathrm{He}}$>6°. A disadvantage is the limited azimuthal acceptance of the BBS, which can drop for specific polar angles of the ^{3}He to less than 10% [Sch97b]. This disadvantage is compensated by the large acceptance of the Plastic Ball for determining the e^-e^+ pairs.

In addition to studying the angular and mass dependence of the $pd \to {}^3\mathrm{He}\, e^+e^-$ reaction, it is planned to perform the experiment at a few incident-beam energies varying between 50 and 200 MeV. At low energies, the real-photon data agree better with the calculations, whereas at higher energies (200 MeV) we have seen that a large discrepancy between data and calculation appears. Therefore, covering the complete energy range might give insight into where the disagreement sets in. In addition, by studying the virtual-photon yield, one gets a handle on all components of the nuclear current.

7.3 Conclusions

7.3.1 The $pp \to ppe^+$

The main part of this the
and response functions o
follows.

- The $pp \to ppe^+e^-$ react
time with a negligible am
of the experimental equip
- The predictions for the
Kor96] and the microscopi
microscopic model overest
calculations, of which the
energies discussed here, gi
- For the first time, an att
into six different componen
photon. For these type of
of the dileptons is require
here, which therefore gave
the achieved accuracy both
a reasonable description o
experiment featuring the
decomposing the cross secti

7.3.2 The $pd \to {}^3\mathrm{He}\,\gamma$

In addition to the $pp \to pp$
iment on the real- and virt
respectively. The results of
- The $pd \to {}^3\mathrm{He}\,\gamma$ experime
added new data to the worl
- The data are compared wi
Kor99]. The model is unde
magnetic moment of the ^{3}He
calculation is reduced signifi
predictions of the model to d
- We have successfully dete
process, $pd \to {}^3\mathrm{He}\, e^+e^-$. Th
spectrometer PACMAN [Joh
- The Uppsala experiment f
photon yield and the real-pho
ment discussed here does not
and predictions for our kinem
- In order to fit the predicti
$^3\mathrm{He}\, e^+e^-$ data, a similar modi
sary as was found in the real-

7.3 Conclusions

7.3.1 The $pp \rightarrow ppe^+e^-$ experiment

The main part of this thesis focussed on the experimental determination of the cross sections and response functions of the $pp \rightarrow ppe^+e^-$ experiment. The results can be summarised as follows.

- The $pp \rightarrow ppe^+e^-$ reaction below pion-production threshold has been measured for the first time with a negligible amount of background and with reasonable statistics. Here, the quality of the experimental equipment plays an important role for the success of the experiment.
- The predictions for the $pp \rightarrow ppe^+e^-$ cross section of the low-energy calculations [Kor95, Kor96] and the microscopic model [Mar97a, Mar97b, Mar98] are compared with the data. The microscopic model overestimates the data significantly. Surprisingly, one of the low-energy calculations, of which the predictions are expected to be outside its range of validity at the energies discussed here, gives a good description of the data.
- For the first time, an attempt has been made to experimentally decompose the cross section into six different components related to the yields for different polarization states of the virtual photon. For these type of studies high statistics and a good coverage of the scattering angles of the dileptons is required. These requirements were not met in the experiment discussed here, which therefore gave partly model-dependent results with large uncertainties. Within the achieved accuracy both models (microscopic and low-energy approximations) seem to give a reasonable description of the experimental data. It is expected that a second-generation experiment featuring the Plastic Ball detector will significantly improve on experimentally decomposing the cross sections into the six components.

7.3.2 The $pd \rightarrow {}^3\mathrm{He}\,\gamma$ and $pd \rightarrow {}^3\mathrm{He}\,e^+e^-$ experiments

In addition to the $pp \rightarrow ppe^+e^-$ results, we presented and discussed the results of an experiment on the real- and virtual-photon capture processes: $pd \rightarrow {}^3\mathrm{He}\,\gamma$ and $pd \rightarrow {}^3\mathrm{He}\,e^+e^-$, respectively. The results of this measurement can be summarised as follows.

- The $pd \rightarrow {}^3\mathrm{He}\,\gamma$ experiment discussed here has determined differential cross sections which added new data to the world database.
- The data are compared with predictions of a gauge-invariant impulse approximation [Kor98, Kor99]. The model is underestimating the data significantly. By increasing the anomalous magnetic moment of the ^{3}He by more than a factor of two, the discrepancy between data and calculation is reduced significantly. A similar modification was found to be necessary to fit the predictions of the model to data from other experiments.
- We have successfully determined differential cross sections of the virtual-photon capture process, $pd \rightarrow {}^3\mathrm{He}\,e^+e^-$. These data are complementary to data obtained with the dilepton-spectrometer PACMAN [Joh98].
- The Uppsala experiment found that at specific kinematics the ratio between the virtual-photon yield and the real-photon yield was enhanced compared with calculations. The experiment discussed here does not find a discrepancy between the experimentally determined ratio and predictions for our kinematics.
- In order to fit the predictions of the gauge-invariant impulse approximation to the $pd \rightarrow {}^3\mathrm{He}\,e^+e^-$ data, a similar modification of the anomalous magnetic moment of the ^{3}He is necessary as was found in the real-photon capture.

• For the first time, an attempt was made to decompose the $pd \rightarrow {}^3\mathrm{He}\, e^+e^-$ cross section into four different components related to the yields for different polarization states of the virtual photon. This introduces new observables which can be used to test the model even further. Only at invariant virtual-photon masses (M_γ<40 MeV) a discrepancy (sign difference) of the interference response function W_{TT} between the prediction of the model and the data is found.

Nederlan

Inleiding

De belangrijkste doelstell
van materie om ons heen.
aan dat de bouwsteen van
wolk van elektronen. Het
kunnen worden in gelade
king bestaat tussen de nu
gevormd. Om de eigensch
de wisselwerking tussen d

Een voor de hand ligg
menteel te bestuderen, is
te laten botsen en de rich
proces, wat bekend staat
figuur 1. Hier botst een p
het aantal verstrooide nuc
meten. Door deze resultat
modellen, kan het beste m
beschrijft, worden geselecte

Om de sterke wisselwerk
zijn elastische verstrooiings
dan twee nucleonen bestaat
worden bestudeerd in het s
de aanwezigheid van de an
zoals zijn massa en ladingsv
proton of neutron. Ter illu
ton weergegeven, wat volge
geladen quarks: twee "up"
figuur 2 is de situatie gesch
onen een andere vorm aanne
in de eigenschappen tussen
actie tussen twee "off-shell"
nucleonen. Dit verschil word
manier om dit soort effecten
te laten botsen, maar waar
geproduceerd. Vanwege ene